

Article

Kinetics of Polymer Network Formation by Nitroxide-Mediated Radical Copolymerization of Styrene/Divinylbenzene in Supercritical Carbon Dioxide

Gabriel Jaramillo-Soto, Samuel Alejandro Sarracino-Silva and Eduardo Vivaldo-Lima * 

Facultad de Química, Departamento de Ingeniería Química, Universidad Nacional Autónoma de México, Ciudad de México 04510, Mexico

* Correspondence: vivaldo@unam.mx

Abstract: The kinetics of nitroxide-mediated dispersion copolymerization with crosslinking of styrene (STY) and divinylbenzene (DVB) in supercritical carbon dioxide (scCO₂) is addressed experimentally. 2,2,6,6-Tetramethylpiperidiny-1-oxy (TEMPO) and dibenzoyl peroxide (BPO) were used as nitroxide controller and initiator, respectively. A high-pressure cell with lateral sapphire windows at 120 °C and 207 bar was used to carry out the polymerizations. The nitroxide-mediated homopolymerization (NMP) of STY, as well as the conventional radical copolymerization (FRC) of STY/DVB, at the same conditions were also carried out as reference and for comparison purposes. The effect of nitroxide content on polymerization rate, evolution of molecular weight averages, gel fraction, and swelling index was studied.

Keywords: reversible-deactivation radical polymerization; nitroxide-mediated polymerization; polymer networks; supercritical carbon dioxide; free radical copolymerization



Citation: Jaramillo-Soto, G.; Sarracino-Silva, S.A.; Vivaldo-Lima, E. Kinetics of Polymer Network Formation by Nitroxide-Mediated Radical Copolymerization of Styrene/Divinylbenzene in Supercritical Carbon Dioxide. *Processes* **2022**, *10*, 2386. <https://doi.org/10.3390/pr10112386>

Academic Editor: Li Xi

Received: 17 October 2022

Accepted: 5 November 2022

Published: 14 November 2022

Publisher's Note: MDPI stays neutral with regard to jurisdictional claims in published maps and institutional affiliations.



Copyright: © 2022 by the authors. Licensee MDPI, Basel, Switzerland. This article is an open access article distributed under the terms and conditions of the Creative Commons Attribution (CC BY) license (<https://creativecommons.org/licenses/by/4.0/>).

1. Introduction

The properties of polymeric materials with tridimensional network structures produced by conventional free radical copolymerization with crosslinking (FRC) of vinyl and divinyl monomers make them relevant for many technological applications. The best performance in these applications is obtained when the materials possess homogeneous structures. Unfortunately, the FRC of vinyl/divinyl monomers usually leads to highly heterogeneous microstructures due to the inherent characteristics of this method, which include slow initiation, fast propagation, high termination rates, and large dispersities (\bar{M}) of the molar mass of primary chains. Cyclization and compositional drift promote the formation of highly compact crosslinked regions mixed with looser ones, which add to the highly heterogeneous nature of polymer networks synthesized by this route [1].

The incorporation of reversible-deactivation radical polymerization (RDRP) controllers during the manufacture of polymer networks by FRC of vinyl/divinyl monomers is reported to reduce the heterogeneity of the materials [2]. Polymer networks with claimed reduced heterogeneity of crosslink density distribution have therefore been synthesized by nitroxide-mediated polymerization (NMP) [3–16], initiator-chain transfer-terminator (INIFERTER) polymerization [16–21], atom transfer radical polymerization (ATRP) [22–31], and reversible addition-fragmentation chain transfer (RAFT) polymerization [32–45]. The first reports using NMP during the synthesis of polymer networks were pioneer reports focused on the synthesis of the materials [3–6], measurement and control of the porosity of the materials [7,8], synthesis in dispersed (mini-emulsion) [9–12] or micro-suspension [13] conditions, generation of reliable kinetic data [14,15], and a review on NMP which includes a comprehensive coverage of this topic [16]. The scope and progress are similar for the other chemistries (INIFERTER, RAFT and ATRP).

The use of compressed fluids as solvents in polymer chemistry gained relevance in the 1990s and the first decade of this century. New developments continue in the present decade. Carbon dioxide at supercritical conditions (scCO₂) is the solvent most extensively used. The replacement of conventional polluting organic solvents by scCO₂ in organic synthesis is important from a non-polluting green chemistry perspective. There are many reports on the synthesis of polymers in scCO₂ as a continuous phase [46–48]. A few reviews on polymer chemistry in scCO₂ are available [47,49–53].

A few years ago, we presented the first reports concerning the production of polymer networks using RDRP chemistries and carried out in scCO₂ [2,54,55]. The examples analyzed included the RAFT copolymerization of styrene (STY) and divinylbenzene (DVB) [54,55], RAFT copolymerization of methyl methacrylate (MMA) and ethylene glycol dimethacrylate (EGDMA) [2,55], and RAFT copolymerization of hydroxyethyl methacrylate (HEMA) and EGDMA [55–57]. We have also modelled these copolymerizations [58].

Although recent studies focused on the synthesis of polymer networks in the presence of RDRP controllers, such as the synthesis of soft, elastomeric, non-tacky polymer networks; combining RAFT synthesis of the network followed by photo-induced ATRP grafting of side chains [59]; the development of a novel class of acrylic acid (AA)-based superabsorbent polymers (SAPs) with improved absorption performance by applying iodine transfer polymerization (ITP) [60]; the assessment of the advantages of RDRP polymer networks over conventional FRC ones for 3D printing [61]; and the development of a photoinduced free radical-promoted cationic RAFT polymerization method using the direct photolysis of the RAFT agent as a radical source, which was further combined with photo-INIFERTER RAFT polymerization to prepare polymer networks [62], have been reported lately (2019–2022), none of them have been carried out in scCO₂, and none of them have used NMP chemistry.

In this contribution we report the nitroxide-mediated copolymerization with crosslinking of STY and DVB in scCO₂ using 2,2,6,6-Tetramethylpiperidine-1-oxy (TEMPO) and dibenzoyl peroxide (BPO) as the nitroxide controller and initiator, respectively. A high-pressure cell with lateral sapphire windows at 120 °C and 207 bar was used as the reaction vessel. The motivation and background for this study is contained in a patent generated in our group [55].

2. Experimental

2.1. Chemicals

STY (Sigma-Aldrich, Naucalpan, México, 99%,) was washed three times using a 10 wt.% NaOH solution and dried for 24 h. with MgSO₄. It was then filtrated, followed by vacuum distillation at 22 °C. DVB (Sigma-Aldrich) was a technical mixture of isomers (p-DVB and m-DVB) with approximately 80 wt.% DVB and was used without further purification. Dibenzoyl peroxide (BPO) (Akzo Nobel Chemicals, Los Reyes La Paz, Mexico, 97 wt.%) was recrystallized twice from methanol. Carbon dioxide (Praxair, Naucalpan, Mexico, 99.99% purity) was used without further purification. TEMPO (Sigma-Aldrich, 99 wt.%) was also used without additional purification steps. Krytox[®] 257 FSL (DuPont, M_n = 2500 g mol⁻¹) was used as a dispersing aid and was not purified.

2.2. Reaction System

The polymerization system, shown in Figure 1, was similar to the one used in our previous systems on (co)polymerizations carried out in sc-CO₂ [2,54,63,64]. The copolymerizations in scCO₂ proceeded in a 38 mL high-pressure cell. A Dual Syringe Pump System was used to feed CO₂ into the vessel and bring it to supercritical conditions. Monomers (8 g), initiator, TEMPO, stabilizer, and a magnetic stirring bar were placed inside the reactor. A slow flow of CO₂ was used to purge the reactor. It was then pressurized with CO₂ until a pre-defined pressure, lower than the desired reaction pressure, was reached. After that, the reactor was heated using heating tape (heating elements distributed homogeneously between flexible molded sheets of silicon) until the set reaction temperature (T = 120 °C) was reached and maintained. Pressure was then increased to the required reaction pres-

sure ($P = 207$ bar) by loading additional CO_2 . The reaction mixture was stirred using the magnetic bar. The polymerization went on until the desired time elapsed.

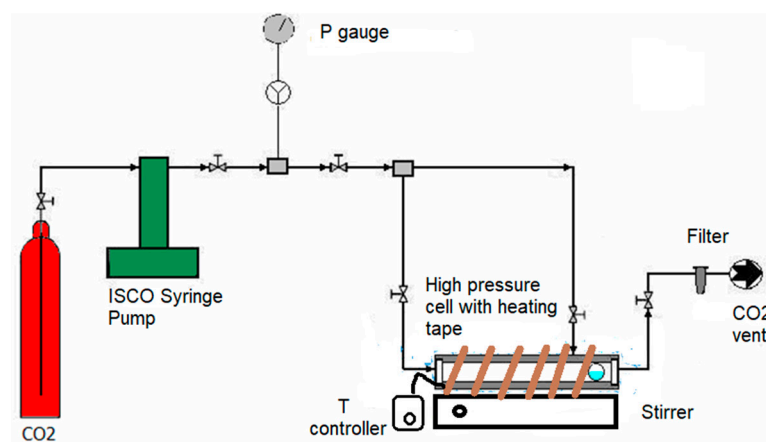


Figure 1. Sketch of the reacting system for NMC of styrene and divinylbenzene in scCO_2 .

2.3. Product Characterization

Monomer conversion was determined from gravimetry. Gel content and Swelling Index (SI) were obtained gravimetrically from mass fractions separated by ultracentrifugation, using the same centrifuge as in our previous study [2]. Centrifugation at 18,000 RPM took place for one hour. Molecular weight averages of the soluble fractions were measured by gel permeation chromatography (GPC). The same GPC equipment described in Jaramillo-Soto et al. [2] was used. THF was filtered and used as the eluent at a flow rate of 1 mL/min. Polymer solutions of ± 0.2 wt.% were prepared and allowed to dissolve for 24 h. They were then micro filtered using injection volumes of 100 to 200 μL .

3. Results and Discussion

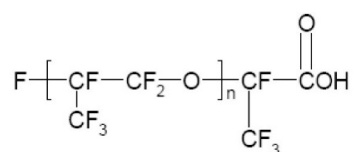
3.1. Operating Conditions and Cases Analyzed

The objective of this study was to analyze the kinetics of polymer network formation by nitroxide mediated copolymerization (NMC) of styrene and divinylbenzene carried out in scCO_2 . FRP and NMP of STY and conventional FRC of STY/DVB were also considered in the study as reference systems useful in the analysis. The polymerizations reported in this study, which are summarized in Table 1, proceeded at a temperature (T) of 120 $^\circ\text{C}$ and pressure (P) of 207 bar, using Krytox 257 FSL as a stabilizer. The chemical structure of Krytox 257 FSL is shown in Scheme 1. As shown in Table 1, eight case studies were considered in this contribution, all carried out in scCO_2 . Case 1 deals with FRP of STY, whereas Case 2 concerns the NMP of STY, and Case 3 refers to conventional FRC of STY/DVB. These three cases are reference cases. Cases 4 to 8 concern the NMC of STY and DVB at different crosslinker and controller concentrations.

Table 1. Cases of homopolymerization of STY and copolymerization of STY/DVB in scCO_2 , either conventional or NMP.

Case	Description	[DVB] (wt.%)	[TEMPO]/[BPO] ^a
1	FRP of STY	0	0
2	NMP of STY	0	1.1
3	FRC of STY/DVB	1	0
4	NMC of STY/DVB	1	1.1
5	NMC of STY/DVB	1.5	1.1
6	NMC of STY/DVB	3	1.1
7	NMC of STY/DVB	1	1.6
8	NMC of STY/DVB	1	3

^a Molar ratio, [BPO] = 1 wt.% (wrt to monomer mixture), $T = 120$ $^\circ\text{C}$, $P = 207$ bar.



Scheme 1. Chemical structure of Krytox 257 FSL.

3.2. Comparison of Base Case of NMC of STY/DVB (Case 4) against Reference Situations (Cases 1–3)

A comparison of a representative formulation of NMC of STY/DVB in scCO_2 (Case 4) against the reference situations of FRP of STY (Case 1), NMP of STY (Case 2), and FRC of STY/DVB (Case 3) is shown in Figure 2. As expected, the slowest case is the NMP of STY (Case 2), where the controller slows down the polymerization rate and there is no crosslinker which accelerates it, and the fastest case corresponds to the conventional FRC of STY/DVB, where opposite conditions prevail. Intermediate between these two are the NMC of STY/DVB (Case 4), which is the second slowest system, and the FRP of STY (Case 1). In this situation, the reduced polymerization rate caused by the controller dominates over the action of the crosslinker.

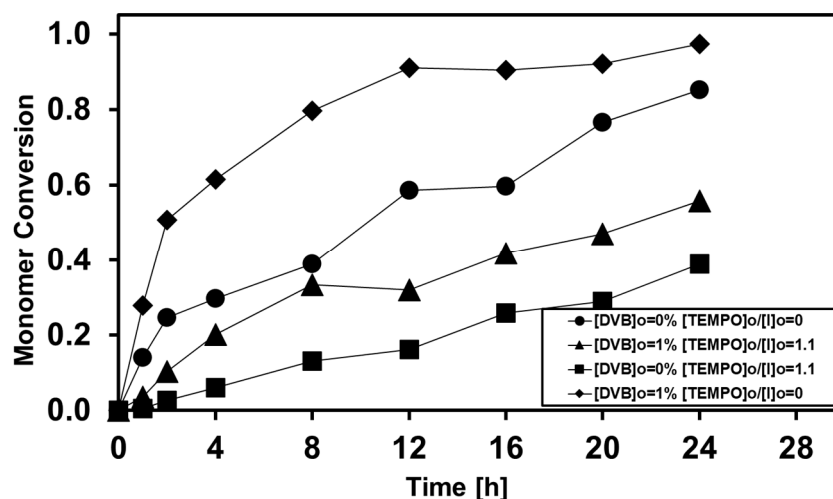


Figure 2. Conversion versus time profiles for the NMC of STY/DVB at $[\text{DVB}] = 1 \text{ wt.}\%$ and $[\text{TEMPO}]/[\text{BPO}] = 1.1$ (triangles) against reference cases of FRP of STY (Case 1, circles), NMP of STY (Case 2, squares), and FRC of STY/DVB (Case 3, diamonds).

3.3. Effect of Crosslinker Content on Polymerization Rate and Evolution of Molecular Weight Averages

The NMC of STY/DVB with a $[\text{TEMPO}]/[\text{BPO}]$ ratio of 1.1 was taken as a base formulation to study the effect of DVB content on the polymerization rate (Figure 3), molecular weight development (Figures 4 and 5), gel fraction versus conversion, and the SI versus conversion. It is observed in Figure 3 that the polymerization proceeds faster as the amount of DVB crosslinker in the formulation is increased.

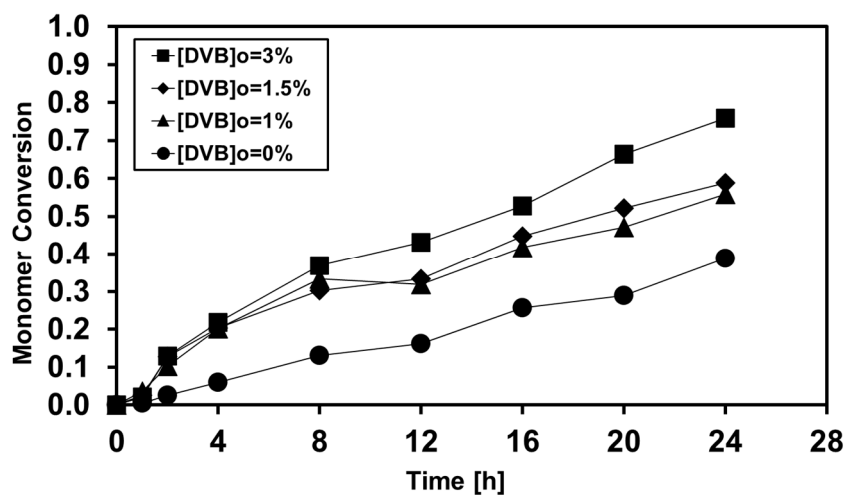


Figure 3. Effect of DVB content on conversion versus time for the NMC of STY/DVB in $scCO_2$ at $[TEMPO]/[BPO] = 1.1$, $T = 120\text{ }^\circ\text{C}$, and $P = 207\text{ bar}$.

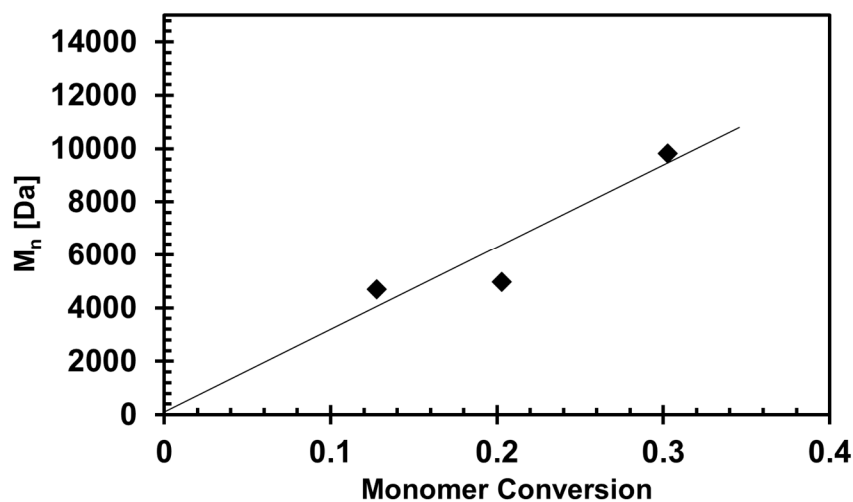


Figure 4. Evolution of M_n for the NMC of STY/DVB in $scCO_2$ at $[TEMPO]/[BPO] = 1.1$, $[DVB] = 1.5\text{ wt.}\%$, $T = 120\text{ }^\circ\text{C}$, and $P = 207\text{ bar}$.

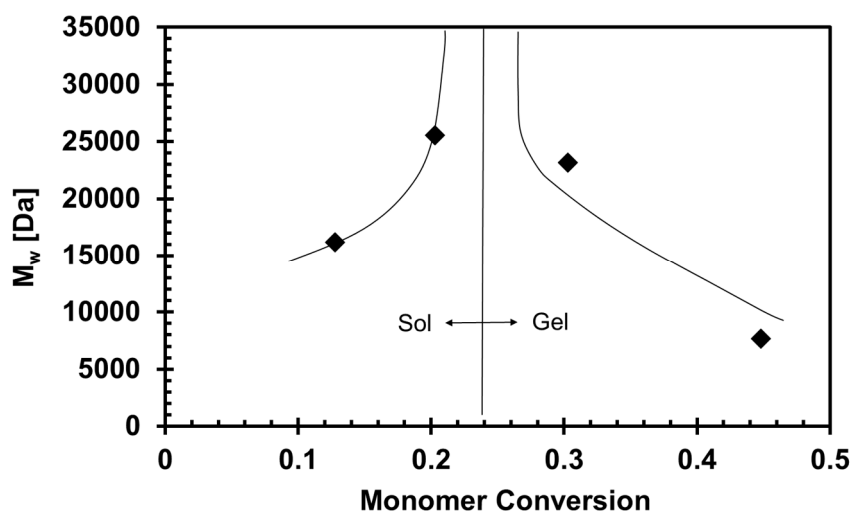


Figure 5. Evolution of M_w for the NMC of STY/DVB in $scCO_2$ at $[TEMPO]/[BPO] = 1.1$, $[DVB] = 1.5\text{ wt.}\%$, $T = 120\text{ }^\circ\text{C}$, and $P = 207\text{ bar}$.

Although not all the samples were characterized for molecular weight development, a linear relationship between number average molecular weight (M_n) and conversion is observed in Figure 4 (see trending line) for Case 5 of Table 1. The data point at 20% monomer conversion seems to deviate from the linear trend. As observed in Figure 5, which shows a plot of weight average molecular weight (M_w) versus conversion, the gelation point occurs precisely between 20% and 25% monomer conversion, a situation that may explain the deviation from the linear trend. It is clearly observed in Figure 5 that M_w increases sharply during the pre-gelation period until the gelation point is reached, and then decreases for the sol fraction during the post-gelation period (see the trending lines), behavior typical for a system with polymer network formation.

Experimental profiles of gel percentage versus monomer conversion at three levels of crosslinker are shown in Figure 6. The exact occurrence of the gelation points is not captured with precision, but the qualitative trend, illustrated by the trending lines, is clear: the gelation point occurs sooner when the concentration of DVB is increased. The gelation point for the system with 3 wt.% DVB content (Case 6) occurs between 5 and 10% monomer conversion; it occurs between 15 and 20% monomer conversion for the system with 1.5 wt.% DVB content (Case 5) and it takes place between 20 and 30% conversion for the system with 1 wt.% DVB content (Case 4). According to Figure 5, the gelation point for Case 4 takes place at about 25% conversion, which agrees with the gelation point observed in Figure 6.

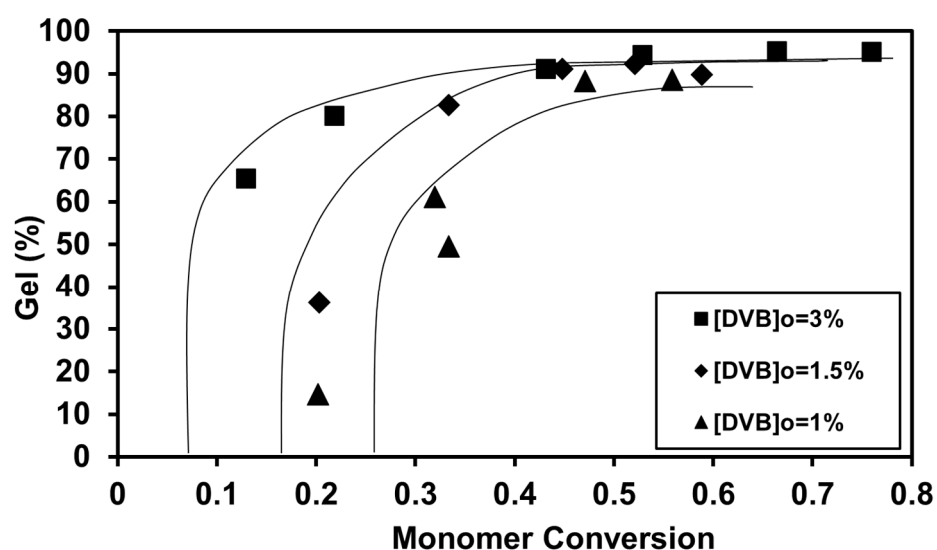


Figure 6. Effect of crosslinker content on gel development for the NMC of STY/DVB in $scCO_2$ at $[TEMPO]/[BPO] = 1.1$, $T = 120\text{ }^\circ\text{C}$, and $P = 207\text{ bar}$.

As shown in Figure 7, the swelling index (SI) is very low before the gelation point. As shown by the trending lines, a sudden increase in the SI around the gel point vicinity and then a gradual decrease after the gelation period is observed for both situations (Cases 4 and 5). Open markers in Figure 7 are repeats of polymerization. Although it is not observed clearly, most of the solid markers are repeats of the measurement for a single sample. These results show that the repeatability of the technique is good, and the reproducibility, understood as replication of the experiments in the same laboratory, is rather large. The gelation points inferred from Figure 7 are slightly higher than those obtained from Figures 5 and 6, but the qualitative trend is correct, since the gelation point at the lower level of crosslinker ($[DVB] = 1\text{ wt.}\%$) occurs later than the corresponding one for the higher level ($[DVB] = 1.5\text{ wt.}\%$).

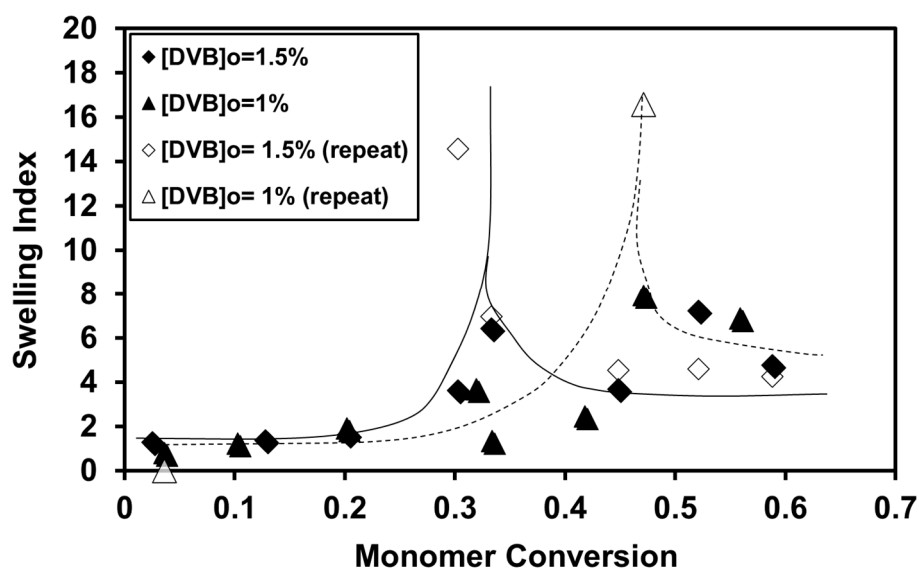


Figure 7. Effect of DVB content on the development of the SI for the NMC of STY/DVB in $scCO_2$ at $[TEMPO]/[BPO] = 1.1$, $T = 120\text{ }^\circ\text{C}$, and $P = 207\text{ bar}$.

3.4. Effect of TEMPO Content on Polymerization Rate and Molecular Weight Development

Cases 3, 4, 7, and 8 of Table 1, all of them with $[DVB] = 1\text{ wt.}\%$, were used to analyze the effect of controller (TEMPO) content on the NMC of STY/DVB at $T = 120\text{ }^\circ\text{C}$ and $P = 207\text{ bar}$. It is observed in Figure 8 that increasing TEMPO content in the reacting mixture results in decreased polymerization rates (slower conversion versus time profiles), a result which is expected in RDRPs.

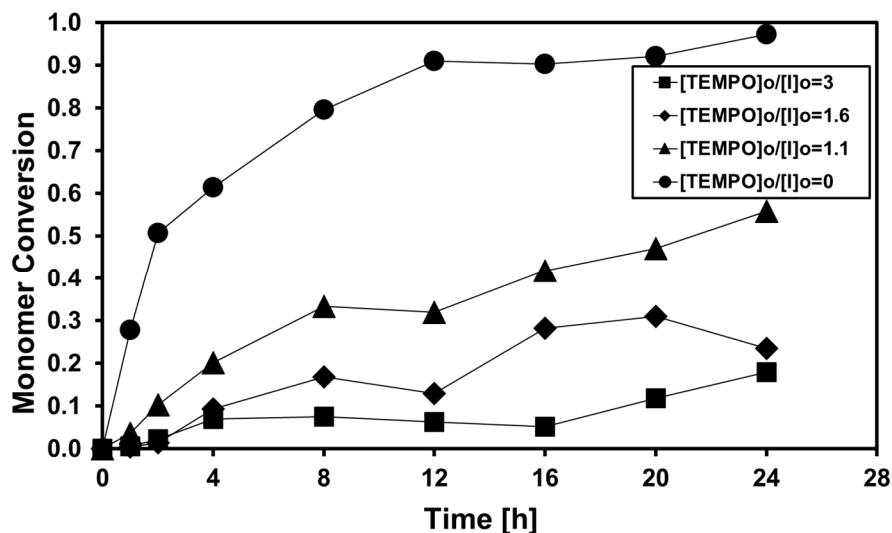


Figure 8. Effect of controller (TEMPO) content on polymerization rate for the NMC of STY/DVB in $scCO_2$ at $[DVB] = 1\text{ wt.}\%$, $T = 120\text{ }^\circ\text{C}$, and $P = 207\text{ bar}$.

It is shown in Figure 9 that the M_n versus conversion (x) profiles for Cases 7 and 8 follow linear trends, with the case with lower TEMPO content reaching slightly higher molecular weights.

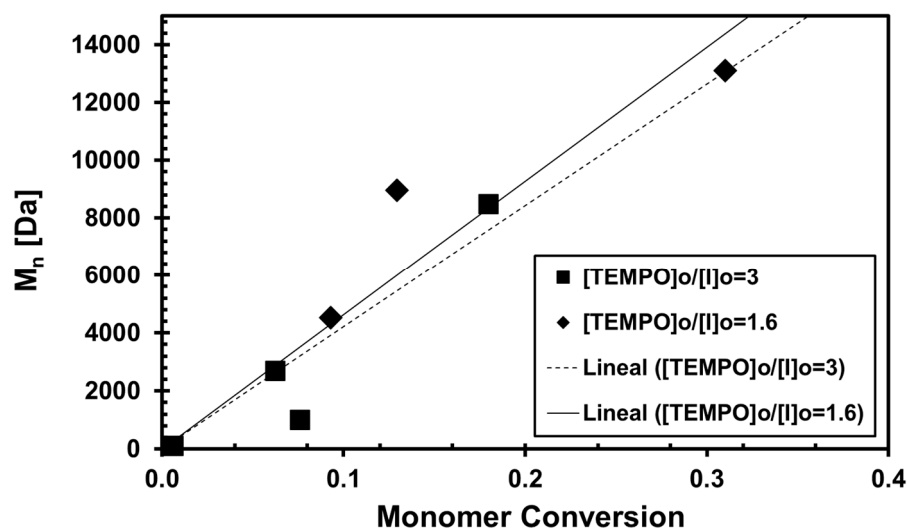


Figure 9. Effect of controller content on the evolution of M_n versus conversion for the NMC of STY/DVB in $scCO_2$ at [DVB] = 1 wt.%, $T = 120\text{ }^\circ\text{C}$, and $P = 207\text{ bar}$.

Figure 10 shows profiles of M_w versus x . At first sight, the data points do not seem to show clear trends. However, when each profile is analyzed individually, the expected trends are revealed. In the case at $[\text{TEMPO}]/[\text{BPO}] = 1.1$, only two data points (triangles) are observed in Figure 10; one of them ($x = 0.1$) seems to correspond to an increasing profile for the pre-gelation period, and the other ($x = 0.33$) to a decreasing profile for the post-gelation period (see solid black trending lines). This indicates that the gelation point for Case 4 occurs between 15 and 25% monomer conversion. In the case at $[\text{TEMPO}]/[\text{BPO}] = 1.6$, there are three data points at conversions lower than 20% monomer conversion, which shows an increasing trend that agrees with the increasing trend of a crosslinking system for the pre-gelation period. The data point at $x = 0.3$ seems to correspond to a decreasing profile for the post-gelation period. This behavior is illustrated with the short-dashed red trending lines. The gelation point for Case 7 occurs between 15 and 28% monomer conversion. In the system at $[\text{TEMPO}]/[\text{BPO}] = 3$ (Case 8), although the data points are scattered, all of them seem to follow the increasing trend of a profile during the pre-gelation period. As indicated by the long-dashed green trending line, it seems that the gelation point was not reached before 24 h, which was the maximum time where samples were taken.

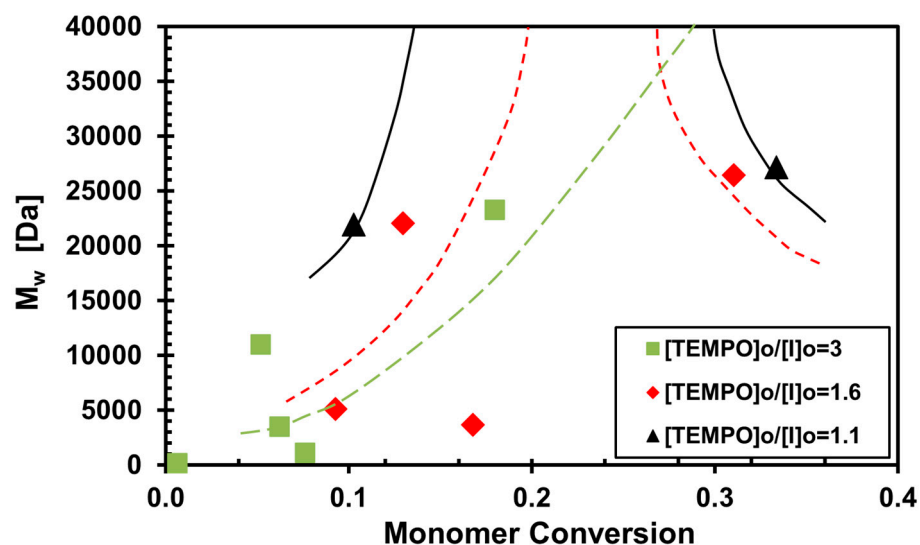


Figure 10. Effect of controller (TEMPO) content on the evolution of M_w versus conversion for the NMC of STY/DVB in $scCO_2$ at [DVB] = 1 wt.%, $T = 120\text{ }^\circ\text{C}$, and $P = 207\text{ bar}$.

Figure 11 shows the profiles of gel percentage versus conversion. As expected, gelation is delayed as the amount of TEMPO is increased. From the data points at low conversions, it can be inferred that the gelation point in the absence of a controller (Case 3) occurs very early during the polymerization (no data point available); gelation occurs between 5 and 10% monomer conversion for Case 4 and between 13 and 25% for Case 7. The colored trending lines of Figure 11 provide an easier way to visualize these results.

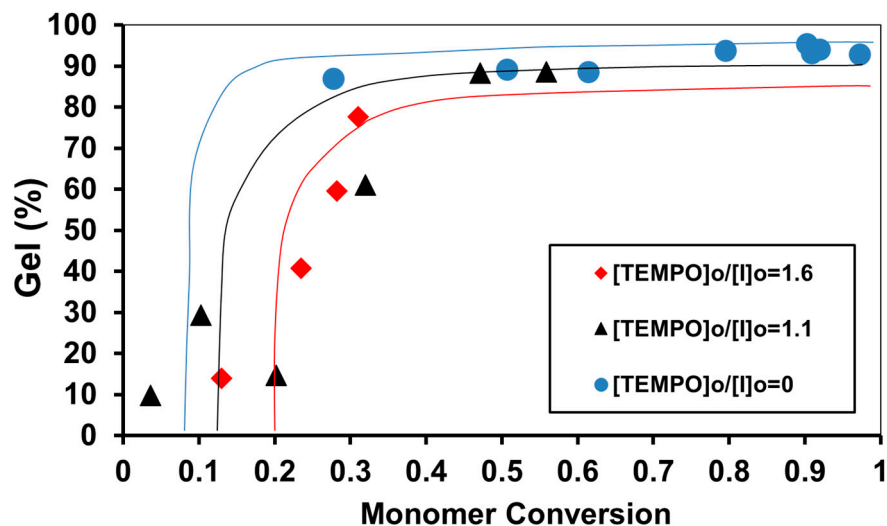


Figure 11. Effect of controller (TEMPO) content on the evolution of gel percentage versus conversion for the NMC of STY/DVB in $scCO_2$ at $[DVB] = 1$ wt.%, $T = 120$ °C, and $P = 207$ bar.

The results of the SI versus conversion shown in Figure 12 confirm that gelation did not take place during the time that the polymerization was monitored in Case 6, the one with $[TEMPO]/[BPO] = 3$ (green trending line and green squares). On the other hand, the SI for Case 7 increased abruptly and then decreased between 20 and 30% monomer conversion, which indicates that gelation took place in that interval, in agreement with what was observed in Figures 10 and 11 (see red trending line and red diamonds).

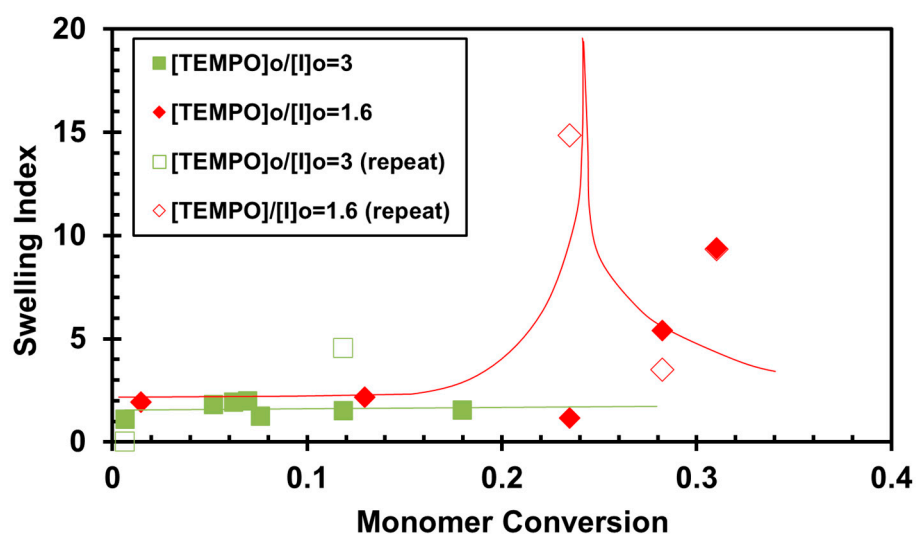


Figure 12. Effect of controller (TEMPO) content on the evolution of the SI versus conversion for the NMC of STY/DVB in $scCO_2$ at $[DVB] = 1$ wt.%, $T = 120$ °C, and $P = 207$ bar. Open symbols are replicates of the experiments.

4. Conclusions

Polymer networks synthesized by FRC of STY/DVB in scCO₂, at 120 °C and 207 bar, in a high-pressure cell with lateral sapphire windows are reported for the first time. The novelty of this process includes the combination of three technological aspects: (a) synthesis of polymer networks; (b) use of RDRP chemistry for the synthesis of controlled polymer microstructures; and (c) the use of scCO₂ as a green route to carry out the polymerization. The results obtained confirmed that crosslinking and gelation took place, that the presence of TEMPO slowed down the polymerization and delayed the occurrence of the gelation point, and that growth was less disordered than in conventional FRC. The reduced rate of polymerization is observed in the conversion versus time profiles, where higher conversions are reached when the amount of TEMPO is reduced. The effect of TEMPO delaying the occurrence of gelation is clearly observed in the M_w versus conversion, SI versus conversion, and gel fraction versus conversion profiles.

The nature of the reactor did not allow obtaining more abundant and precise experimental data but did allow us to prove the concept that we proposed earlier for RAFT copolymerization of STY/DVB in scCO₂ [2,54,55] to the case of NMC of vinyl/divinyl monomers in scCO₂. Namely, polymer networks with different kinetic behavior during the polymerization (slower polymerization rates and delayed gelation) and less heterogeneous crosslink density distributions are obtained when TEMPO is used as a controller, and the material is easily dried by depressurization of the reactor. Our experimental data do not provide direct information on the homogeneity of the polymer network, but the linear relationship between M_n and conversion suggests that less heterogeneous are indeed produced when TEMPO is included in the formulation. This is an issue that requires further analysis in future studies on the topic.

5. Patents

The contents of this manuscript are related to the scope of patent MX/a/2013/009053: “Polímeros con estructura de red de baja densidad y proceso de obtención de los mismos mediante polimerización radicalica por desactivación reversible en fluidos comprimidos” (Low density polymer networks and their production process by reversible-deactivation radical polymerization in compressed fluids), E. Vivaldo-Lima, M. J. Bernad Bernad, A. Licea-Claverie, H. Vázquez-Torres, P. Pérez-Salinas, A. Rosas-Aburto; Date of application: 6/August/2013; Date granted: 13/08/2020 (Filing certificate: MX/E/2020/029514; Título: 377687).

Author Contributions: Conceptualization, E.V.-L.; methodology, E.V.-L. and G.J.-S.; experimental work, G.J.-S. and S.A.S.-S.; formal analysis, G.J.-S. and E.V.-L.; investigation, E.V.-L. and G.J.-S.; resources, E.V.-L.; data curation, G.J.-S., S.A.S.-S. and E.V.-L.; writing—original draft preparation, G.J.-S.; writing—review and editing, E.V.-L.; supervision, E.V.-L.; project administration, E.V.-L.; funding acquisition, E.V.-L. All authors have read and agreed to the published version of the manuscript.

Funding: This research was funded by: (a) Dirección General de Asuntos del Personal Académico, Universidad Nacional Autónoma de México (DGAPA-UNAM), Project PAPIIT IG100122, granted to E.V.-L.; and (b) Facultad de Química, UNAM, research funds granted to E.V.-L. (PAIP 5000-9078). The APC was waived.

Data Availability Statement: The data presented in this study are available on request from the corresponding author.

Acknowledgments: We are indebted to Prof. Alex Penlidis, from the University of Waterloo, for allowing E.V.-L. to check the manuscript for similarity through his UW external academic affiliation.

Conflicts of Interest: The authors declare no conflict of interest. The funders had no role in the design of the study; in the collection, analyses, or interpretation of data; in the writing of the manuscript; or in the decision to publish the results.

References

1. Hernández-Ortiz, J.C.; Vivaldo-Lima, E. Chapter 9: Crosslinking. In *Handbook of Polymer Synthesis, Characterization and Processing*; Saldivar-Guerra, E., Vivaldo-Lima, E., Eds.; John Wiley & Sons: New York, NY, USA, 2013. [\[CrossRef\]](#)
2. Jaramillo-Soto, G.; Villa-Ávila, C.M.; Vivaldo-Lima, E. RAFT Copolymerization with Crosslinking of Methyl Methacrylate and Ethylene Glycol Dimethacrylate in Supercritical Carbon Dioxide. *J. Macromol. Sci. Pure Appl. Chem.* **2013**, *50*, 281–286. [\[CrossRef\]](#)
3. Ide, N.; Fukuda, T. Nitroxide-Controlled Free-Radical Copolymerization of Vinyl and Divinyl Monomers. Evaluation of Pendant-Vinyl Reactivity. *Macromolecules* **1997**, *30*, 4268–4271. [\[CrossRef\]](#)
4. Ide, N.; Fukuda, T. Nitroxide-Controlled Free-Radical Copolymerization of Vinyl and Divinyl Monomers. 2. Gelation. *Macromolecules* **1999**, *32*, 95–99. [\[CrossRef\]](#)
5. Abrol, S.; Kambouris, P.A.; Looney, M.G.; Solomon, D.H. Studies on microgels, 3. Synthesis using living free radical polymerization. *Macromol. Rapid Commun.* **1997**, *18*, 755–760. [\[CrossRef\]](#)
6. Abrol, S.; Caulfield, M.J.; Qiao, G.G.; Solomon, D.H. Studies on microgels. 5. Synthesis of microgels via living free radical polymerization. *Polymer* **2001**, *42*, 5987–5991. [\[CrossRef\]](#)
7. Peters, E.C.; Svec, F.; Fréchet, J.N.J.; Viklund, C.; Irgum, K. Control of Porous Properties and Surface Chemistry in “Molded” Porous Polymer Monoliths Prepared by Polymerization in the Presence of TEMPO. *Macromolecules* **1999**, *32*, 6377–6379. [\[CrossRef\]](#)
8. Viklund, C.; Nordström, A.; Irgum, K.; Svec, F.; Fréchet, J.M.J. Preparation of Porous Poly(styrene-co-divinylbenzene) Monoliths with Controlled Pore Size Distributions Initiated by Stable Free Radicals and Their Pore Surface Functionalization by Grafting. *Macromolecules* **2001**, *34*, 4361–4369. [\[CrossRef\]](#)
9. Zetterlund, P.B.; Alam, M.N.; Minami, H.; Okubo, M. Nitroxide-Mediated Controlled/Living Free Radical Copolymerization of Styrene and Divinylbenzene in Aqueous Miniemulsion. *Macromol. Rapid Commun.* **2005**, *26*, 955–960. [\[CrossRef\]](#)
10. Alam, M.N.; Zetterlund, P.B.; Okubo, M. Network Formation in Nitroxide-Mediated Radical Copolymerization of Styrene and Divinylbenzene in Miniemulsion. *Macromol. Chem. Phys.* **2006**, *207*, 1732–1741. [\[CrossRef\]](#)
11. Saka, Y.; Zetterlund, P.B.; Okubo, M. Gel formation and primary chain lengths in nitroxide-mediated radical copolymerization of styrene and divinylbenzene in miniemulsion. *Polymer* **2007**, *48*, 1229–1236. [\[CrossRef\]](#)
12. Tanaka, T.; Suzuki, T.; Saka, Y.; Zetterlund, P.B.; Okubo, M. Mechanical properties of cross-linked polymer particles prepared by nitroxide-mediated radical polymerization in aqueous micro-suspension. *Polymer* **2007**, *48*, 3836–3843. [\[CrossRef\]](#)
13. Hirano, T.; Tanaka, K.; Wang, H.; Seno, M.; Sato, T. Effect of nitrobenzene on initiator-fragment incorporation radical polymerization of divinylbenzene with dimethyl 2,2'-azobisisobutyrate. *Polymer* **2005**, *46*, 8964–8972. [\[CrossRef\]](#)
14. Tuinman, E.; McManus, N.T.; Roa-Luna, M.; Vivaldo-Lima, E.; Lona, L.M.F.; Penlidis, A. Controlled Free-Radical Copolymerization Kinetics of Styrene and Divinylbenzene by Bimolecular NMRP using TEMPO and BPO. *J. Macromol. Sci. Pure Appl. Chem.* **2006**, *43*, 995–1011. [\[CrossRef\]](#)
15. Nogueira, T.R.; Lona, L.M.F.; McManus, N.T.; Vivaldo-Lima, E.; Penlidis, A. Nitroxide-mediated radical copolymerization of styrene and divinylbenzene: Increased polymerization rate by using TBEC as initiator. *J. Mater. Sci.* **2010**, *45*, 1878–1884. [\[CrossRef\]](#)
16. Vivaldo-Lima, E.; Jaramillo-Soto, G.; Penlidis, A. Nitroxide-mediated polymerization (NMP). In *Encyclopedia of Polymer Science and Technology*; Mark, H.F., Ed.; John Wiley & Sons: New York, NY, USA, 2016. [\[CrossRef\]](#)
17. Kannurpatti, A.R.; Lu, S.; Bunker, G.M.; Bowman, C.N. Kinetic and Mechanistic Studies of Iniferter Photopolymerizations. *Macromolecules* **1996**, *29*, 7310–7315. [\[CrossRef\]](#)
18. Kannurpatti, A.R.; Anderson, K.J.; Anseth, J.W.; Bowman, C.N. Use of “living” radical polymerizations to study the structural evolution and properties of highly crosslinked polymer networks. *J. Polym. Sci. Part B Polym. Phys.* **1997**, *35*, 2297–2307. [\[CrossRef\]](#)
19. Kannurpatti, A.R.; Anseth, J.W.; Bowman, C.N. A study of the evolution of mechanical properties and structural heterogeneity of polymer networks formed by photopolymerizations of multifunctional (meth)acrylates. *Polymer* **1998**, *39*, 2507–2513. [\[CrossRef\]](#)
20. Ward, J.H.; Peppas, N.A. Kinetic Gelation Modeling of Controlled Radical Polymerizations. *Macromolecules* **2000**, *33*, 5137–5142. [\[CrossRef\]](#)
21. Singh, A.; Kuksenok, O.; Johnson, J.A.; Balazs, A.C. Tailoring the structure of polymer networks with iniferter-mediated photo-growth. *Polym. Chem.* **2016**, *7*, 2955–2964. [\[CrossRef\]](#)
22. Asgarzadeh, F.; Ourdouillie, P.; Beyou, E.; Chaumont, P. Synthesis of Polymer Networks by “Living” Free Radical Polymerization and End-Linking Processes. *Macromolecules* **1999**, *32*, 6996–7002. [\[CrossRef\]](#)
23. Jiang, C.; Shen, Y.; Zhu, S.; Hunkeler, D. Gel formation in atom transfer radical polymerization of 2-(N,N-dimethylamino)ethyl methacrylate and ethylene glycol dimethacrylate. *J. Polym. Sci. Part A Polym. Chem.* **2001**, *39*, 3780–3788. [\[CrossRef\]](#)
24. Yu, Q.; Zeng, F.; Zhu, S. Atom Transfer Radical Polymerization of Poly(ethylene glycol) Dimethacrylate. *Macromolecules* **2001**, *34*, 1612–1618. [\[CrossRef\]](#)
25. Yu, Q.; Zhang, J.; Cheng, M.; Zhu, S. Kinetic Behavior of Atom Transfer Radical Polymerization of Dimethacrylates. *Macromol. Chem. Phys.* **2006**, *207*, 287–294. [\[CrossRef\]](#)
26. Li, Y.; Armes, S.P. Synthesis and Chemical Degradation of Branched Vinyl Polymers Prepared via ATRP: Use of a Cleavable Disulfide-Based Branching Agent. *Macromolecules* **2005**, *38*, 8155–8162. [\[CrossRef\]](#)
27. Wang, A.R.; Zhu, S. Branching and gelation in atom transfer radical polymerization of methyl methacrylate and ethylene glycol dimethacrylate. *Polym. Eng. Sci.* **2005**, *45*, 720–727. [\[CrossRef\]](#)

28. Wang, A.R.; Zhu, S. Control of the polymer molecular weight in atom transfer radical polymerization with branching/crosslinking. *J. Polym. Sci. Part A Polym. Chem.* **2005**, *43*, 5710–5714. [[CrossRef](#)]
29. Tsarevsky, N.V.; Matyjaszewski, K. Combining Atom Transfer Radical Polymerization and Disulfide/Thiol Redox Chemistry: A Route to Well-Defined (Bio)degradable Polymeric Materials. *Macromolecules* **2005**, *38*, 3087–3092. [[CrossRef](#)]
30. Gao, H.; Min, K.; Matyjaszewski, K. Determination of Gel Point during Atom Transfer Radical Copolymerization with Cross-Linker. *Macromolecules* **2007**, *40*, 7763–7770. [[CrossRef](#)]
31. Gao, H.; Li, W.; Matyjaszewski, K. Synthesis of Polyacrylate Networks by ATRP: Parameters Influencing Experimental Gel Points. *Macromolecules* **2008**, *41*, 2335–2340. [[CrossRef](#)]
32. Crescenzi, V.; Dentini, M.; Bontempo, D.; Masci, G. Hydrogels based on pullulan derivatives crosslinked via a “living” free-radical process. *Macromol. Chem. Phys.* **2002**, *203*, 1285–1291. [[CrossRef](#)]
33. Barner, L.; Li, C.; Hao, X.; Stenzel, M.H.; Barner-Kowollik, C.; Davis, T.P. Synthesis of core-shell poly(divinylbenzene) microspheres via reversible addition fragmentation chain transfer graft polymerization of styrene. *J. Polym. Sci. Part A Polym. Chem.* **2004**, *42*, 5067–5076. [[CrossRef](#)]
34. Norisuye, T.; Morinaga, T.; Tran-Cong-Miyata, Q.; Goto, A.; Fukuda, T.; Shibayama, M. Comparison of the gelation dynamics for polystyrenes prepared by conventional and living radical polymerizations: A time-resolved dynamic light scattering study. *Polymer* **2005**, *46*, 1982–1994. [[CrossRef](#)]
35. Liu, B.; Kazlauciusas, A.; Guthrie, J.T.; Perrier, S. One-Pot Hyperbranched Polymer Synthesis Mediated by Reversible Addition Fragmentation Chain Transfer (RAFT) Polymerization. *Macromolecules* **2005**, *38*, 2131–2136. [[CrossRef](#)]
36. Liu, B.; Kazlauciusas, A.; Guthrie, J.T.; Perrier, S. Influence of reaction parameters on the synthesis of hyperbranched polymers via reversible addition fragmentation chain transfer (RAFT) polymerization. *Polymer* **2005**, *46*, 6293–6299. [[CrossRef](#)]
37. Krasia, T.C.; Patrickios, C.S. Amphiphilic Polymethacrylate Model Co-Networks: Synthesis by RAFT Radical Polymerization and Characterization of the Swelling Behavior. *Macromolecules* **2006**, *39*, 2467–2473. [[CrossRef](#)]
38. Achilleos, M.; Krasia-Christoforou, T.; Patrickios, C.S. Amphiphilic Model Conetworks Based on Combinations of Methacrylate, Acrylate, and Styrenic Units: Synthesis by RAFT Radical Polymerization and Characterization of the Swelling Behavior. *Macromolecules* **2007**, *40*, 5575–5581. [[CrossRef](#)]
39. Liu, Q.; Zhang, P.; Qing, A.; Lan, Y.; Lu, M. Poly(N-isopropylacrylamide) hydrogels with improved shrinking kinetics by RAFT polymerization. *Polymer* **2006**, *47*, 2330–2336. [[CrossRef](#)]
40. Lin, Y.; Liu, X.; Li, X.; Zhan, J.; Li, Y. Reversible addition–fragmentation chain transfer mediated radical polymerization of asymmetrical divinyl monomers targeting hyperbranched vinyl polymers. *J. Polym. Sci. Part A Polym. Chem.* **2007**, *45*, 26–40. [[CrossRef](#)]
41. Dong, Z.-M.; Liu, X.-H.; Lin, Y.; Li, Y.-S. Branched polystyrene with abundant pendant vinyl functional groups from asymmetric divinyl monomer. *J. Polym. Sci. Part A Polym. Chem.* **2008**, *46*, 6023–6034. [[CrossRef](#)]
42. Yu, Q.; Zhu, Y.; Ding, Y.; Zhu, S. Reaction Behavior and Network Development in RAFT Radical Polymerization of Dimethacrylates. *Macromol. Chem. Phys.* **2008**, *209*, 551–556. [[CrossRef](#)]
43. Roa-Luna, M.; Jaramillo-Soto, G.; Castañeda-Flores, P.V.; Vivaldo-Lima, E. Copolymerization Kinetics of Styrene and Divinylbenzene in the Presence of S-Thiobenzoyl Thioglycolic Acid as RAFT Agent. *Chem. Eng. Technol.* **2010**, *33*, 1893–1899. [[CrossRef](#)]
44. López-Domínguez, P.; Hernández-Ortiz, J.C.; Barlow, K.J.; Vivaldo-Lima, E.; Moad, G. Modeling the Kinetics of Monolith Formation by RAFT Copolymerization of Styrene and Divinylbenzene. *Macromol. React. Eng.* **2014**, *8*, 706–722. [[CrossRef](#)]
45. Moad, G. RAFT (Reversible addition–fragmentation chain transfer) crosslinking (co)polymerization of multi-olefinic monomers to form polymer networks. *Polym. Int.* **2015**, *64*, 15–24. [[CrossRef](#)]
46. Canelas, D.A.; DeSimone, J.M. Polymerizations in Liquid and Supercritical Carbon Dioxide. *Adv. Polym. Sci.* **1997**, *133*, 103–140.
47. Kendall, J.L.; Canelas, D.A.; Young, J.L.; DeSimone, J.M. Polymerizations in Supercritical Carbon Dioxide. *Chem. Rev.* **1999**, *99*, 543–564. [[CrossRef](#)]
48. Charpentier, P.A.; Kennedy, K.A.; DeSimone, J.M.; Roberts, G.W. Continuous Polymerizations in Supercritical Carbon Dioxide: Chain-Growth Precipitation Polymerizations. *Macromolecules* **1999**, *32*, 5973–5975. [[CrossRef](#)]
49. Kemmere, M.F. Supercritical Carbon Dioxide for Sustainable Polymer Processes. In *Supercritical Carbon Dioxide in Polymer Reaction Engineering*; Kemmere, M.F., Meyer, T., Eds.; Wiley-VCH: Weinheim, Germany, 2005.
50. Harrisson, S.; Liu, X.; Ollagnier, J.-N.; Coutelier, O.; Marty, J.-D.; Destarac, M. RAFT Polymerization of Vinyl Esters: Synthesis and Applications. *Polymers* **2014**, *6*, 1437–1488. [[CrossRef](#)]
51. Zhao, H. Enzymatic ring-opening polymerization (ROP) of polylactones: Roles of non-aqueous solvents. *J. Chem. Technol. Biotechnol.* **2018**, *93*, 9–19. [[CrossRef](#)]
52. Tsai, W.-C.; Wang, Y. Progress of supercritical fluid technology in polymerization and its applications in biomedical engineering. *Prog. Polym. Sci.* **2019**, *98*, 101161. [[CrossRef](#)]
53. Fan, Y.; Picchioni, F. Modification of starch: A review on the application of “green” solvents and controlled functionalization. *Carbohydr. Polym.* **2020**, *241*, 116350. [[CrossRef](#)]
54. Jaramillo-Soto, G.; Vivaldo-Lima, E. RAFT copolymerization of styrene/divinylbenzene in supercritical carbon dioxide. *Aust. J. Chem.* **2012**, *65*, 1177–1185. [[CrossRef](#)]

55. Vivaldo-Lima, E.; Bernad-Bernad, M.J.; Licea-Claverie, A.; Vázquez-Torres, H.; Pérez-Salinas, P.; Rosas-Aburto, A. Low Density Polymer Networks and Their Production Process by Reversible Deactivation Radical Polymerization in Compressed Fluids. Mexican Patent MX/a/2013/009053, 13 August 2020.
56. Pérez-Salinas, P.; Rosas-Aburto, A.; Antonio-Hernández, C.H.; Jaramillo-Soto, G.; Vivaldo-Lima, E.; Licea-Claverie, A.; Castro-Ceseña, A.B.; Vázquez-Torres, H. Controlled Release of Vitamin B-12 using Hydrogels Synthetized by Free Radical and RAFT Copolymerization in scCO₂. *Macromol. Symp.* **2016**, *360*, 69–77. [[CrossRef](#)]
57. Pérez-Salinas, P.; Jaramillo-Soto, G.; Rosas-Aburto, A.; Vázquez-Torres, H.; Bernad-Bernad, M.J.; Licea-Claverie, A.; Vivaldo-Lima, E. Comparison of Polymer Networks Synthesized by Conventional Free Radical and RAFT Copolymerization Processes in Supercritical Carbon Dioxide. *Processes* **2017**, *5*, 26. [[CrossRef](#)]
58. López-Domínguez, P.; Hernández-Ortiz, J.C.; Vivaldo-Lima, E. Modeling of RAFT Copolymerization with Crosslinking of Styrene/Divinylbenzene in Supercritical Carbon Dioxide. *Macromol. Theory Simul.* **2018**, *27*, 1700064. [[CrossRef](#)]
59. Cuthbert, J.; Martinez, M.R.; Sun, M.; Flum, J.; Li, L.; Olszewski, M.; Wang, Z.; Kowalewski, T.; Matyjaszewski, K. Non-Tacky Fluorinated and Elastomeric STEM Networks. *Macromol. Rapid Commun.* **2019**, *40*, 1800876. [[CrossRef](#)]
60. Miyajima, T.; Matsubara, Y.; Komatsu, H.; Miyamoto, M.; Suzuki, K. Development of a superabsorbent polymer using iodine transfer polymerization. *Polym. J.* **2020**, *52*, 365–373. [[CrossRef](#)]
61. Bagheri, A.; Fellows, C.M.; Boyer, C. Reversible Deactivation Radical Polymerization: From Polymer Network Synthesis to 3D Printing. *Adv. Sci.* **2021**, *8*, 2003701. [[CrossRef](#)]
62. Zhao, B.; Li, J.; Li, Z.; Lin, X.; Pan, X.; Zhang, Z.; Zhu, J. Photoinduced 3D Printing through a Combination of Cationic and Radical RAFT Polymerization. *Macromolecules* **2022**, *55*, 7181–7192. [[CrossRef](#)]
63. García-Morán, P.R.; Jaramillo-Soto, G.; Albores-Velasco, M.E.; Vivaldo-Lima, E. An Experimental Study on the Free-Radical Copolymerization Kinetics with Crosslinking of Styrene and Divinylbenzene in Supercritical Carbon Dioxide. *Macromol. React. Eng.* **2009**, *3*, 58–70. [[CrossRef](#)]
64. Jaramillo-Soto, G.; García-Morán, P.R.; Enríquez-Medrano, F.J.; Maldonado-Textle, H.; Albores-Velasco, M.E.; Guerrero-Santos, R.; Vivaldo-Lima, E. Effect of stabilizer concentration and controller structure and composition on polymerization rate and molecular weight development in RAFT polymerization of styrene in supercritical carbon dioxide. *Polymer* **2009**, *50*, 5024–5030. [[CrossRef](#)]